

See discussions, stats, and author profiles for this publication at:
<https://www.researchgate.net/publication/228452893>

High resolution photoionisation spectroscopy of vibrationally excited Ar·NO

ARTICLE *in* CHEMICAL PHYSICS LETTERS · JANUARY 2001

Impact Factor: 1.9 · DOI: 10.1016/S0009-2614(00)01359-2

CITATIONS

11

READS

9

4 AUTHORS, INCLUDING:



Timothy P Softley

University of Oxford

105 PUBLICATIONS 1,789 CITATIONS

SEE PROFILE



Stuart R Mackenzie

University of Oxford

82 PUBLICATIONS 1,232 CITATIONS

SEE PROFILE

High resolution photoionisation spectroscopy of vibrationally excited Ar·NO

O.L.A. Monti^a, H.A. Cruse^a, T.P. Softley^{a,*}, S.R. Mackenzie^b

^a *Physical and Theoretical Chemistry Laboratory, University of Oxford, South Parks Road, Oxford OX1 3QZ, UK*

^b *Department of Chemistry, University of Warwick, Coventry CV4 7AL, UK*

Received 16 October 2000; in final form 13 November 2000

Abstract

Mass-analysed threshold ionisation (MATI) spectra of the Ar·NO complex have been obtained for the first time. These spectra have been used to determine unambiguously the nature of three bands detected by resonance-enhanced multiphoton ionisation (REMPI) spectroscopy via the \tilde{A} state of Ar·NO. The features are shown to originate from vibrationally excited states of Ar·NO in its electronic ground state. The assignment is in agreement with recent theoretical calculations. © 2001 Elsevier Science B.V. All rights reserved.

1. Introduction

The study of weakly bound complexes has attracted considerable interest in the recent past, both from the point of view of spectroscopy [1,2] and dynamics [3,4]. A small number of molecular systems, such as Ar·NO [5–18], have been the subject of intense research. The shallow well of the intermolecular potential in van der Waals molecules creates an interesting regime between molecular scattering and traditional spectroscopy. Van der Waals complexes such as Ar·NO are of particular interest due to the subtle influences of the various coupled angular momenta, and open-shell van der Waals molecules remain in the focus of current research [19].

Experimentally, seminal work by Levy and co-workers on Ar·NO [20] using laser-induced fluorescence has led to a series of studies of electronically excited states such as the \tilde{A} state [9–13] and the \tilde{C} state [15]. Obi and coworkers found a barrier of 24 cm⁻¹ to dissociation on the excited state surface [9]. This in turn allowed the dissociation energy, $D_0' = 88$ cm⁻¹, in the ground state of Ar·NO to be determined. In two recent publications [13,14], Wright and coworkers presented a detailed analysis of the $\tilde{A} \leftarrow \tilde{X}$ spectra, identifying a series of vibrational progressions to states with excitation of the van der Waals bending and stretching modes. The same group also investigated the Ar·NO⁺ cation using zero-kinetic-energy pulsed-field ionisation (ZEKE-PFI) spectroscopy [13]. Due to large changes in the van der Waals bond length and angle on ionisation, a number of long vibrational progressions were observed and attributed to the van der Waals modes of the ion.

* Corresponding author. Fax: +44-0-1865-275-410.

E-mail address: tim.softley@chemistry.ox.ac.uk (T.P. Softley).

From a theoretical point of view, $\text{Ar} \cdot \text{NO}$ has proved to be one of the milestones in the study of weakly bound systems. Howard et al. [8] presented a Hamiltonian to analyse spectra arising from excitation of end-over-end motion of asymmetric tops in ${}^2\Pi$ states. Fawzy and Hougen extended this description to account for the full rotational motion and to generalise to ${}^{2S+1}A \leftarrow {}^{2S+1}A$ and ${}^{2S+1}A + 1 \leftarrow {}^{2S+1}A$ transitions [21]. However, the model excludes large-amplitude motion. This aspect has been addressed by Hutson and coworkers [22] in an alternative formalism, considering the perturbing effect of the potential anisotropy on the free rotation of the diatomic, but in turn neglecting end-over-end motion. In a series of publications, Alexander et al. calculated the potential energy surface (PES) in the electronic ground state at various levels of theory [6,16], the highest level being CCSD(T) extrapolated to the complete basis-set limit. They determined the energies of the lowest rovibronic levels [17,18], the integral inelastic scattering cross-sections [6] and very recently the energies and wave functions of the lower bound bend-stretch levels [5]. This work provides a solid basis for detailed experimental investigations.

Here we present an experimental study of the lowest vibrational states of $\text{Ar} \cdot \text{NO}$ in its electronic ground state by $(1 + 1')$ resonance-enhanced multiphoton ionisation (REMPI) spectroscopy. Three bands observed to the red of the origin band are unambiguously assigned for the first time to vibrationally excited $\text{Ar} \cdot \text{NO}$ on the basis of mass-analysed threshold ionisation (MATI) spectra. These observations are closely related to the overtone spectra reported by Meyer and coworkers [5]. The MATI spectra constitute the first of their kind for $\text{Ar} \cdot \text{NO}$. With its high species selectivity, MATI spectroscopy, the mass-selective analogue of ZEKE-PFI spectroscopy, is rapidly emerging as a powerful tool in gas-phase chemical physics, both in spectroscopy, as evidenced in this work, and in reaction dynamics [23–27].

2. Experimental

The experimental set-up has been described in detail previously [27]. It relies on excitation of

rotationally cold $\text{Ar} \cdot \text{NO}$ in either a $1 + 1'$ REMPI or MATI scheme. After direct ionisation (REMPI) or delayed pulsed-field ionisation (MATI) the $\text{Ar} \cdot \text{NO}^+$ ions are accelerated by a series of electrodes and dynodes and are detected by a pair of multi-channel plates.

Briefly, the apparatus consists of a differentially pumped skimmer chamber, operating at 10^{-5} mbar, and the main chamber, containing an arrangement of ion optics. A gas mixture of Ar (BOC, $\geq 99.995\%$) and nitric oxide (MG Gases, $\geq 99.5\%$), 0.5–10% molar fraction of NO, at stagnation pressures of 2–7 bar, is expanded through a nozzle (General Valve, 1 mm diameter) to form a 10 Hz pulsed supersonic expansion. When recording dilution curves, the gas mixture is balanced in Ne (BOC, CP grade) at constant total pressure. The expansion is introduced into the main chamber through a 0.5 mm skimmer. We routinely obtain rotational temperatures of 2 K as estimated from $\text{Ar} \cdot \text{NO}$ and NO REMPI spectra.

In both the $1 + 1'$ REMPI and the $1 + 1'$ MATI schemes, the first step of the excitation is in the vicinity of the $\tilde{A} \, {}^2\Sigma^+(v' = 0) \leftarrow \tilde{X} \, {}^2\Pi_{1/2}(v'' = 0)$ transition of free NO. Two laser beams are introduced collinearly into the main chamber and gently focussed using a 15 cm cylindrical fused-silica lens. The beams intersect the molecular beam perpendicularly. The frequency-tripled (BBO) output of a Nd:YAG-pumped dye-laser (Spectron 4000G/SL800, 10 Hz, 8 ns pulse length) with a Pyridine-1/DCM dye solution is used for the $\tilde{A} \leftarrow \tilde{X}$ excitation (~ 226 nm, 300 μJ per pulse). The transition to high- n Rydberg states (MATI) or into the ionisation continuum (REMPI) is excited by the doubled (KDP) output of a second Nd:YAG-pumped dye laser (Spectron 4000G/SL800, Pyridine-1/DCM dye mixture, ~ 330 nm, 2 mJ per pulse). To discriminate against NO detection in the REMPI studies, the second laser is set to a wavelength that is insufficient for ionisation of rotationally cold NO molecules present in the supersonic expansion. Both lasers are calibrated by a pulsed wavemeter (Burleigh WA 4500).

As in Fig. 1 of Ref. [27], the molecules are excited between the skimmer plate at ground potential and a fine mesh (Buckbee-Mears, 45 lines per inch), kept at -5 V for REMPI detection. The

excited molecules enter a second region defined by the first grid and a further mesh electrode 25 mm beyond the first one. For the purposes of REMPI detection, a small acceleration field is applied across this region, following a short voltage pulse of +300 V applied to the second electrode. The pulse is carefully timed so as to repel the fast NO ions formed by *single colour* resonant ionisation while leaving the heavier $\text{Ar}\cdot\text{NO}$ ions unaffected, as the latter are still in the first field region. Additional discrimination is provided by gating the detection assembly, thus allowing for exclusive detection of $\text{Ar}\cdot\text{NO}$. A further mesh and a dynode stack serve to accelerate the ions towards the detector. In the case of MATI detection, a small repelling field (ca. 450 mV/cm) between the skimmer plate and the first electrode is switched on 3 μs after excitation so as to repel any prompt ions. Care is taken to employ as small a repelling field as possible to avoid inducing fast autoionisation and predissociation processes in the Rydberg-tagged complexes. A small field of 5 V/cm between the first two meshes is used for pulsed-field ionisation of the high- n Rydberg states of $\text{Ar}\cdot\text{NO}$. The remainder of the experiment is identical to the REMPI set-up. The ions are detected by a pair of matched multi-channel plates (MCPs, Gallileo) in Chevron configuration, gated by a fast high-voltage pulse to detect only the desired $\text{Ar}\cdot\text{NO}$ ions. The MCPs are coupled to a phosphor screen and the signal is recorded by use of a conventional photomultiplier tube (PMT), then amplified and processed by a boxcar integrator and an analogue-to-digital converter. The resulting spectra are recorded by a PC.

3. Results and discussion

We report here MATI spectra originating from previously uncharacterised bands in the $\tilde{A} \leftarrow \tilde{X}$ REMPI spectrum of $\text{Ar}\cdot\text{NO}$ and assign the REMPI bands unambiguously to transitions from vibrationally excited $\text{Ar}\cdot\text{NO}$ in the ground electronic state. Fig. 1 shows the spectrum over the whole region. We observe the same features as reported by Wright et al. [13], with the main peaks labelled A, B and C. In addition to this structure,

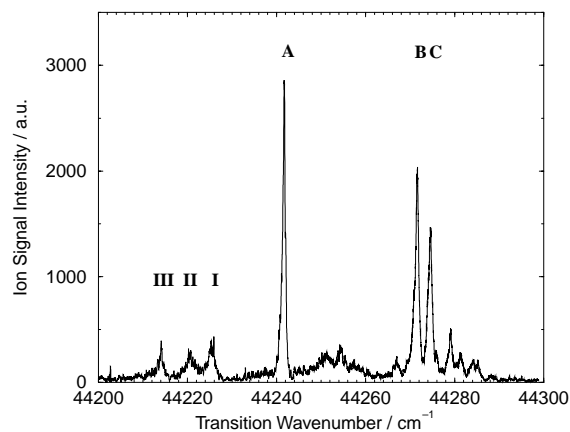


Fig. 1. $1 + 1'$ REMPI spectrum of $\text{Ar}\cdot\text{NO}$. Bands A, B and C and some of the smaller bands in the region between 44 240 and 44 300 cm^{-1} have been observed and assigned previously [13]. Bands I–III are shown in Fig. 1 of reference [12] but are assigned here for the first time to transitions from vibrationally excited levels in the electronic ground state of $\text{Ar}\cdot\text{NO}$.

we find three features, henceforth labelled I, II and III, *to the red* of the origin band, peak A. These bands appear at -15 , -21 and -27 cm^{-1} relative to the origin band. They are slightly broader than the main peaks in the spectrum, indicating either a higher rotational temperature, a higher moment of inertia of the corresponding species or a more complex band system.

In previous work, band contour simulations within the framework of a rigid-rotor model have been used to obtain effective rotational constants for peaks A to C. Following this procedure and using previously published rotational constants [7,13], we obtained good fits to the band contours of peaks A to C. They gave a rotational temperature of 2 K (see Fig. 2), in good agreement with the rotational temperature obtained from band contour simulations for NO under similar conditions. The fact that such an approach has severe deficiencies is highlighted when fitting peaks I–III. The band contours proved to be very sensitive to the effective rotational constants $\bar{B}'' = \frac{1}{2}(B'' + C'')$ for the \tilde{X} state and $\bar{B}' = \frac{1}{2}(B' + C')$ for the \tilde{A} state. They were found to be (in pairs of (\bar{B}', \bar{B}'')) (0.034, 0.040 cm^{-1}) for I/II and (0.027, 0.030 cm^{-1}) for III. These values are in reasonable agreement with those reported for the main transitions A, B and C

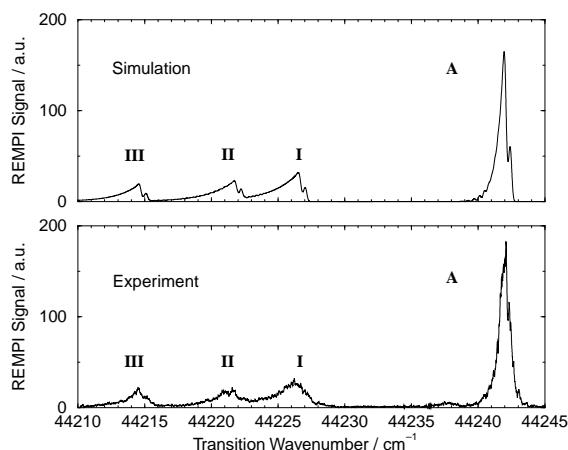


Fig. 2. Experimentally observed REMPI spectrum and band contour simulations for bands A and I–III based on a simple rigid-rotor model. Band A was simulated with a rotational temperature of $T_{\text{rot}} = 2\text{K}$ and effective rotational constants (\bar{B}' , \bar{B}'') of (0.040, 0.070 cm^{-1}). Bands I–III were simulated with $T_{\text{rot}} = 10\text{K}$ and the following effective rotational constants: (0.034, 0.040 cm^{-1}) for bands I/II and (0.027, 0.030 cm^{-1}) for band III.

of $\text{Ar} \cdot \text{NO}$ [13], e.g. for band A (0.04, 0.07 cm^{-1}). However, satisfactory fits could only be obtained with a rotational temperature of 10 K. The values of the effective rotational constants need to be accepted with caution in the light of the assignment presented later in this work. For example, band II is likely to be a superposition of two band systems and theoretical calculations [5] suggest that a simple rigid-rotor model is unlikely to be successful. The fits indicate though that the lower states of transitions I–III have longer bond lengths than in the vibrational ground state.

When the bands I–III were first observed, several possibilities for their origin needed to be considered. The main ones were:

1. The bands correspond to transitions in the REMPI spectrum of $(\text{NO})_2$.
2. The bands originate from larger $\text{Ar}_m \cdot (\text{NO})_n$ clusters leading to $\text{Ar} \cdot \text{NO}$ production by boil-off.
3. The absorption takes place from excited ground-state $\text{Ar} \cdot \text{NO}$.

Some features in this spectral region have been reported previously, but with varying interpretations. Miller raised the possibility that the origin

band is to be found at 44 223 cm^{-1} [11], while bands I–III are faintly observed in the spectrum reported by McQuaid and coworkers [12]. However, in the latter work the authors stated ‘no feature ascribable to $\text{Ar} \cdot \text{NO}$ was observed in [the] region [near the A–X band origin of NO]’. Furthermore, other features in the region of bands I–III were presumed to be associated with higher-order clusters of Ar and NO. Bush et al. mentioned [13] other features thought to arise from either vibrationally excited $\text{Ar} \cdot \text{NO}$ or from fragmentation of larger clusters. Their spectra however do not extend to the region of bands I–III.

The time-of-flight mass-resolution is sufficient to rule out categorically NO as a source of the unknown bands, but it does not allow clean separation of $(\text{NO})_2$ and $\text{Ar} \cdot \text{NO}$. Detection of NO dimer ions can be discounted on other grounds. As has been argued previously [28], two-photon excitation of $(\text{NO})_2$ in this spectral region proceeds via a dissociative intermediate state and no NO dimer ions can be detected. Note also that the $(\text{NO})_2^+$ accessed with the wavelengths used is predissociative and would lead to the detection of NO^+ rather than the dimer ion.

With regard to possibility 2, Fig. 3 shows the integrated band intensity of peaks I–III relative to peak A, as a function of stagnation pressure and Ar concentration. These relative measurements take into account changes in rotational temperature and concentration of the $\text{Ar} \cdot \text{NO}$ species. For all three peaks, no significant change in relative intensity with backing pressure or with Ar concentration was observed. Error bars for such measurements are rather large owing to the difficulty of accurately measuring high and low pressures using the same mixing line. Dilution curves varying the NO concentration show no change either – beyond fluctuations within the noise level – in the intensity of features I–III relative to band A. With bands I–III showing the same dependence on pressure and dilution as band A, we interpret these findings as evidence against bands I–III corresponding to transitions in higher-order clusters.

We investigated the nature of the red-shifted bands I–III further by recording a series of MATI spectra. ZEKE spectra of $\text{Ar} \cdot \text{NO}$ via peaks A and B

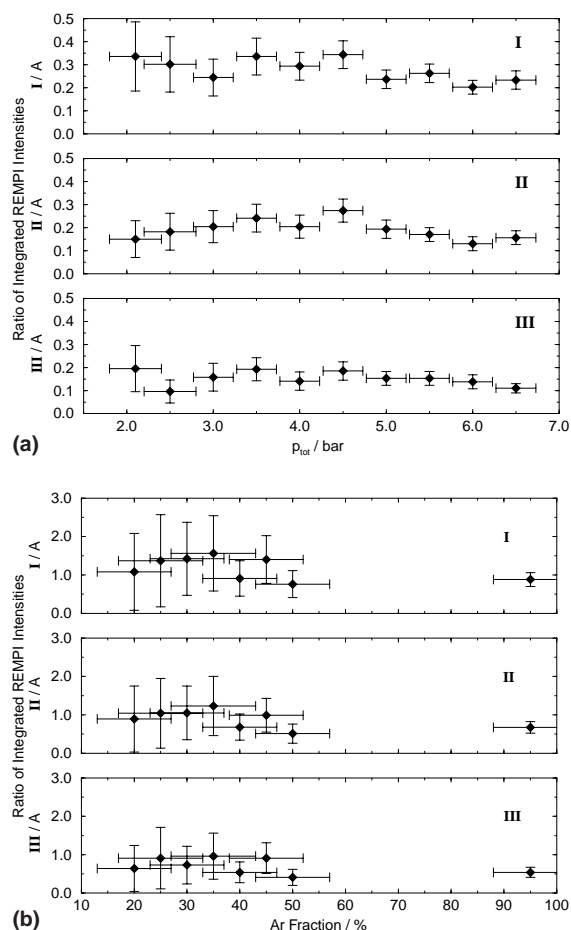


Fig. 3. (a) Integrated intensities of bands I–III relative to band A as a function of total backing pressure. The fraction of NO in the mixture is 2.5%. (b) Integrated intensities of bands I–III relative to band A as a function of Ar fraction in a mixture with 5% NO, balanced in Ne at a backing pressure of 4 bar. No significant change in these ratios is observed for either the curve of growth or the dilution curve, indicating that bands I–III are not due to a species of the type $\text{Ar}_m \cdot \text{NO}_n$, $m, n > 1$.

have been reported previously [13]. The various decay channels available to the high- n Rydberg states of molecules, such as autoionisation and predissociation, in conjunction with the long time-of-flight necessary for satisfactory mass-selection, require careful choice of the excitation conditions for MATI spectroscopy, such as electric field and background ion densities (for a discussion of these issues see Ref. [27]). The MATI data presented here constitute the first of their kind for $\text{Ar} \cdot \text{NO}$.

Fig. 4 shows a comparison of the MATI spectra obtained via peak A and via peak I. All the MATI spectra were obtained by keeping the wavelength of the tripled dye laser fixed on the relevant transition in the REMPI spectrum (≈ 229 nm) and scanning the doubled dye laser only. Comparison of our MATI spectrum via peak A and the ZEKE spectrum reported by Wright and coworkers shows identical vibrational progressions in the ionic state of $\text{Ar} \cdot \text{NO}$. Recording the MATI spectra via the weak spectroscopic features I–III proved to be a formidable challenge, with only a very small number of Rydberg states detected per laser shot. The overall intensity of the observed features varied to some extent in the course of the day, since the small count rates necessitated very slow scanning and long averages. It is clear however that the two MATI spectra in Fig. 4 display an identical series of peaks. Similar spectra were obtained for all three features I–III, as shown in Fig. 5. When comparing the absolute position of the vibrational peaks, i.e. the sum of the tripled and the doubled dye laser wave numbers, in the MATI spectra via bands I–III with those via peak A, we found that the spectra were red-shifted by

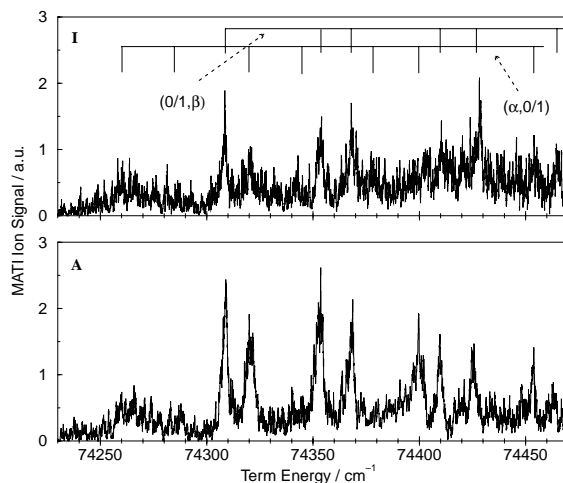


Fig. 4. Comparison of the MATI spectra recorded via band A and via band I. Assignments are given in terms of two modes α and β , corresponding at low energy to the van der Waals stretching vibration and the van der Waals bending vibration of the ion. The relative intensities vary between the two spectra due to low count rates of high- n Rydberg states.

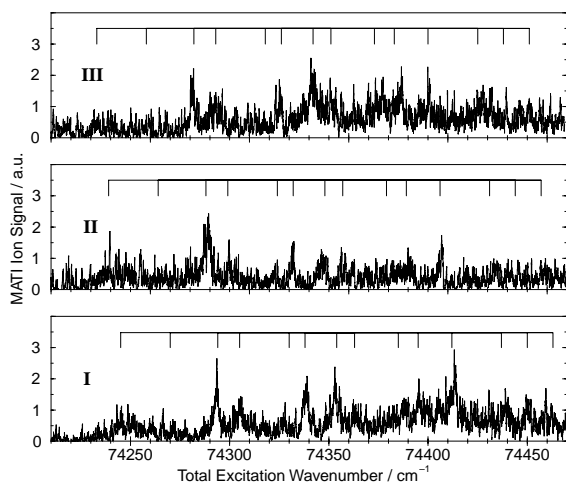


Fig. 5. Comparison of the MATI spectra via bands I–III. The rake in each of the spectra indicates the transitions to all observed ionic vibrational levels. The same bands are present in all three spectra, shifted in energy by -15 , -21 , and -27 cm^{-1} relative to those in the MATI spectrum via band A.

the same amount as the features in the REMPI spectrum. Therefore, the intermediate state must be at the same energy in each case and I–III correspond to excitation from vibrationally excited $\text{Ar}\cdot\text{NO}$ in the \tilde{X} state to the linear vibrational origin in the \tilde{A} state. This conclusion is fully consistent with the band contour analysis, the appearance of the growth and dilution curves and the structure of the MATI spectra for peaks I–III.

Very recently high-level *ab initio* calculations of the first few vibrationally excited levels of the ground state of $\text{Ar}\cdot\text{NO}$ were presented in a publication by Kim et al. [5] using the CCSD(T) potential energy surface. The calculations predict a dissociation energy of 83.2 cm^{-1} , in excellent agreement with experiment. Their calculations were compared with IR-overtone spectra of $\text{Ar}\cdot\text{NO}$ (\tilde{X} , $P = 1/2$, $v_{\text{NO}} = 0$, $v_{\text{b}} = 0$, $v_{\text{s}} = 0$) \rightarrow $\text{Ar}\cdot\text{NO}$ (\tilde{X} , P' , $v_{\text{NO}} = 2$, v'_{b} , v'_{s}), recorded using $(2+1)$ REMPI detection in the vicinity of the \tilde{F} and \tilde{H} electronic states of NO. P is the projection quantum number of the total angular momentum on the $\text{Ar}\cdot\text{NO}$ intramolecular axis and v_{NO} , v_{b} , v_{s} are the vibrational quantum numbers of the intramolecular NO stretching vibration, the van der Waals bending vibration and the van der Waals stretching vibration, respectively. It was found

that the observed bands, labelled B, C and D in their work, are *blue-shifted* from the $v_{\text{NO}} = 0 \rightarrow v_{\text{NO}} = 2$ origin band A by approximately 4, 15 and 20 cm^{-1} , respectively. These shifts are in excellent agreement with the ground state, $v_{\text{NO}} = 0$, level structure calculated using the CCSD(T) potential surface. This allowed assignment of the bands to the excited levels of $v_{\text{NO}} = 2$, if very weak coupling between the NO stretching vibration and the van der Waals modes is assumed. The calculated energies relative to the lowest state of $\text{Ar}\cdot\text{NO}$, effectively corresponding to transitions B, C and D, are as follows:

B: $P = 3/2$, $v_{\text{s}} = 0$, $v_{\text{b}} = 1$	3.72/4.16 cm^{-1} ,
C: $P = 1/2$, $v_{\text{s}} = 0$, $v_{\text{b}} = 1$	13.77/14.94 cm^{-1} ,
D: $P = 1/2$, $v_{\text{s}} = 1$, $v_{\text{b}} = 0$	19.78/19.98 cm^{-1} ,
$P = 3/2$, $v_{\text{s}} = 0$, $v_{\text{b}} = 2$	20.73/21.24 cm^{-1} .

The energy levels given are the lowest calculated rotational states for each almost doubly degenerate, Renner–Teller split level.

In the present work we observe *red shifts* of -15 , -21 , and -27 cm^{-1} for bands I–III. Bands I and II can therefore be assigned to excitation out of the van der Waals excited levels with $v_{\text{NO}} = 0$, analogous to bands C and D in the infrared-overtone work. Furthermore, using the same level of theory, Alexander predicts [29] the $P = 3/2$, $v_{\text{s}} = 1$, $v_{\text{b}} = 1$ level to lie at $26.4/27.9$ cm^{-1} , in good agreement with our observation, allowing the assignment of a transition from this level to band III.

It is interesting to note that the observation of these hot bands in our work implies that the vibrational and rotational temperatures in the beam are very different. Note also that the rotational constants obtained from the band contour simulations are *effective* rotational constants only, including the effects of overlapping bands and a simplistic model Hamiltonian.

4. Conclusion

We have characterised three bands in the REMPI spectrum of $\text{Ar}\cdot\text{NO}$ in the vicinity of the $\tilde{A} \leftarrow \tilde{X}$ transition of NO. We were able to assign the features to transitions from vibrationally excited levels in the electronic ground state of $\text{Ar}\cdot\text{NO}$, consistent with recent high-level

calculations [5,29]. For the first time, MATI spectra via the \tilde{A} state of Ar·NO have been recorded. The use of MATI spectroscopy proved to be crucial in the identification of the nature of bands I–III. It would be of interest to record these observed bands at high resolution to test further the theoretical understanding of the ground state of Ar·NO. The spectroscopy of excited van der Waals complexes allows accurate modelling of these highly flexible and loosely bound molecules, sampling the bound region of the intermolecular scattering surface.

Acknowledgements

Valuable discussions with T.G. Wright and M.H. Alexander are gratefully acknowledged. O.L.A.M. would like to acknowledge Merton College, Oxford for a Greendale Senior Scholarship and the PTCL Oxford for financial aid. This work has been supported by the EPSRC under grant GR/L18303.

References

- [1] M.C. Heaven, *J. Phys. Chem.* 97 (1993) 8567.
- [2] K. Müller-Dethlefs, P. Hobza, *Chem. Rev.* 100 (2000) 143.
- [3] M.I. Lester, *Adv. Chem. Phys.* 96 (1996) 51.
- [4] E.R. Bernstein, *Annu. Rev. Phys. Chem.* 46 (1995) 197.
- [5] Y. Kim, J. Fleniken, H. Meyer, M.H. Alexander, P.J. Dagdigian, *J. Chem. Phys.* 113 (2000) 73.
- [6] M.H. Alexander, *J. Chem. Phys.* 99 (1993) 7725.
- [7] P.D.A. Mills, C.M. Western, B.J. Howard, *J. Phys. Chem.* 90 (1986) 4961.
- [8] P.D.A. Mills, C.M. Western, B.J. Howard, *J. Phys. Chem.* 90 (1986) 3331.
- [9] K. Tsuji, K. Shibuya, K. Obi, *J. Chem. Phys.* 100 (1994) 5441.
- [10] J.C. Miller, W.-C. Cheng, *J. Phys. Chem.* 89 (1985) 1647.
- [11] J.C. Miller, *J. Chem. Phys.* 90 (1989) 4031.
- [12] M.J. McQuaid, G.W. Lemire, R.C. Sausa, *Chem. Phys. Lett.* 227 (1994) 54.
- [13] A.M. Bush, J.M. Dyke, P. Mack, D.M. Smith, T.G. Wright, *J. Chem. Phys.* 108 (1998) 406.
- [14] J. Lozeille, S.D. Gamblin, S.E. Daire, T.G. Wright, D.M. Smith, *J. Chem. Phys.* 113 (2000) 7224.
- [15] P. Mack, J.M. Dyke, D.M. Smith, T.G. Wright, H. Meyer, *J. Chem. Phys.* 109 (1998) 4361.
- [16] M.H. Alexander, *J. Chem. Phys.* 111 (1999) 7426.
- [17] T. Schmelz, P. Rosmus, M.H. Alexander, *J. Phys. Chem. A* 98 (1994) 1073.
- [18] M.H. Alexander, *J. Chem. Phys.* 111 (1999) 7435.
- [19] Y. Kim, K. Patton, J. Fleniken, H. Meyer, *Chem. Phys. Lett.* 318 (2000) 522.
- [20] P.R.R. Langridge-Smith, E.M. Carrasquillo, D.H. Levy, *J. Chem. Phys.* 74 (1981) 6513.
- [21] W.M. Fawzy, J.T. Hougen, *J. Mol. Spectrosc.* 137 (1989) 154.
- [22] M.-L. Dubernet, D. Flower, J.M. Hutson, *J. Chem. Phys.* 94 (1991) 7602.
- [23] F. Merkt, S.R. Mackenzie, T.P. Softley, *J. Chem. Phys.* 99 (1993) 4213.
- [24] S.R. Mackenzie, T.P. Softley, *J. Chem. Phys.* 101 (1994) 10609.
- [25] T.P. Softley, S.R. Mackenzie, F. Merkt, D. Rolland, *Adv. Chem. Phys.* 101 (1997) 667.
- [26] H. Xu, N.E. Shafer-Ray, F. Merkt, D.J. Hughes, M. Springer, R.P. Tuckett, R.N. Zare, *J. Chem. Phys.* 103 (1995) 5157.
- [27] O.L.A. Monti, H. Dickinson, S.R. Mackenzie, T.P. Softley, *J. Chem. Phys.* 112 (2000) 3699.
- [28] K. Sato, Y. Achiba, K. Kimura, *Chem. Phys. Lett.* 126 (1986) 306.
- [29] M.H. Alexander, Private communication.